Available online at www.sciencedirect.com
SCIENCE DIRECT®
International Journal of Heat and Mass Transfer 47 (2004) 2785–2794
International Journal of HEAT and MASS TRANSFER
www.elsevier.com/locate/ijhmt

Conjugate free convection from a vertical plate fin with a rounded tip embedded in a porous medium

A.Z. Vaszi [a], L. Elliott [b], D.B. Ingham [b], I. Pop [c,*]

[a] Rock Deformation Research, School of Earth Sciences, University of Leeds, Leeds LS2 9JT, UK
[b] Department of Applied Mathematics, University of Leeds, Leeds LS2 9JT, UK
[c] Faculty of Mathematics, University of Cluj, R-3400 Cluj, CP 253, Romania

Received 21 October 2003

Abstract

In this paper the two-dimensional conjugate free convection in a porous medium is investigated from a vertical plate fin. Both physically and mathematically it is important to consider a smooth profile for the tip of the fin, such as a rounded tip of an arbitrary shape. Such fin shapes approximate well the rectangular fin, and their study allows a more accurate prediction of the heat transfer quantities, since no restrictive conditions have to be imposed, such as an insulated tip, and there are no singularities appearing in the mathematical formulation.

The governing equations of the convective flow in the porous medium are coupled to the governing equation for the heat flow in the fin by the conditions of continuity of the temperature and the heat flux at the solid/porous media interface. The governing non-dimensional parameters are the convection–conduction parameter, N_{cc}, and the aspect ratio of the fin, λ.

Keywords: Natural convection; Conjugate; Boundary-layer; Vertical fin; Porous medium

1. Introduction

Research in convective heat transfer from fins embedded in viscous fluids or porous media has been intensified in recent years. This is a result of the recognition of the necessity of accurate solution methodologies in various technological applications, such as heat transfer analysis of extended surfaces, geothermal systems, etc. It has been found that the heat transfer coefficient is not invariant along the surface of fins, see [1,2], but it has to be obtained as part of the solution procedure of the coupled conduction–convection, conjugate heat transfer problem. Different types of conjugate problems are well documented in the books by Nield and Bejan [3] and Pop and Ingham [4], and the book by Sunden and Heggs [5] presents an overview of the problems related to heat transfer for fin type surfaces.

The conjugate free convection from a vertical fin embedded in a porous medium has been analysed by integral, finite-difference and local non-similarity methods, and Pop and Nakayama [6] provide an excellent review on this problem. Liu and Minkowycz [7] and Liu et al. [8] studied the natural convection from a plate and cylindrical shaped fin, respectively, and they assumed that the heat conduction in the fin is one-dimensional along the axis of the fin. Vaszi et al. [9] extended the analysis on both of these papers by considering two-dimensional heat conduction in the fin and solving the conjugate problem by a finite-difference approach. In their work they assumed the tip of the fin to be insulated, and they also investigated the validity of this boundary condition.

In this paper we investigate the conjugate free convection in a porous medium from a vertical rectangular

* Corresponding author. Tel.: +40-264-194315; fax: +40-264-591906.
E-mail addresses: attila@rdr.leeds.ac.uk (A.Z. Vaszi), popi@math.ubbcluj.ro (I. Pop).

0017-9310/$ - see front matter © 2004 Elsevier Ltd. All rights reserved.
doi:10.1016/j.ijheatmasstransfer.2004.01.001

Nomenclature

a, b	thickness and length of the fin, respectively
F, G, η	similarity variables
g	magnitude of the acceleration due to gravity
h	local heat transfer coefficient
k_f, k_s	thermal conductivity of the porous medium and the solid fin, respectively
$\bar{k}$	k_s/k_f
K	permeability of the isotropic porous medium
N_{cc}	conduction–convection parameter
q	local heat flux
Q	total heat transfer rate from the fin
Ra	Rayleigh number, $\frac{gK\beta\rho_\infty(T_c-T_\infty)b}{\alpha\mu}$
T	temperature
T_c	constant temperature at the base of the fin
T_f, T_s	temperature of the porous medium and the solid fin, respectively
U, V	velocity components along the X and Y axes, respectively
X, x	dimensional and non-dimensional distance along the surface of the fin, respectively
Y, y	dimensional and non-dimensional distance normally outwards from the fin, respectively
$\bar{y}$	non-dimensional distance normal to the surface of the fin, measured in the fin

Greek symbols

α	effective thermal diffusivity of the porous medium
$\bar{\alpha}$	angle between the Y-axis and the downward vertical
β	coefficient of the thermal expansion
θ_f, θ_s	non-dimensional temperature of the porous medium and the solid fin, respectively
λ	aspect ratio of the rectangular part of the fin
μ	dynamic viscosity of the fluid
ρ	density of the fluid
Ψ, ψ	dimensional and non-dimensional stream-function, respectively

Subscripts

circ, rect	reference to the circular and rectangular parts of the fin, respectively
d	dimensional quantities
∞	reference value at a large distance from the fin

plate fin heated at its base, whose tip ends in a smooth profile, as would occur in practice. In order to illustrate the computational procedure, we have taken the end of the fin to be half of a cylinder of diameter the width of the rectangular section of the fin, thus extending the problem of free convection from a vertical plate fin studied by Vaszi et al. [9]. The two-dimensional heat conduction in the fin is coupled to the convection boundary-layer in the porous medium by the conditions of the continuity of the temperature and the heat flux at the porous medium–solid interface. The boundary-layer starts at the lowest point on the fin, and it gradually grows in thickness along the cylindrical tip and then along the main body of the fin as the base of the fin is approached. Similarity transformations are possible to employ for the boundary-layer along the fin from the tip to the base, and no singularity appears in the mathematical formulation. These similarity transformations were introduced by Merkin [10] for the free convection boundary-layer around an isothermal cylinder surrounded by a porous medium. In the case of fins with a flat tip, Vaszi et al. [9] employed the artificial, but frequently assumed, boundary condition of an insulating fin tip, which may be restrictive, and it introduces mathematical inaccuracies when dealing with the heat and fluid flow in the vicinity of the tip in practical situations. These authors also studied analytically the mathematical singularity that appears at the fin surface near the fin tip which, of course, does not occur in practice and the present work avoids it.

Several theoretical investigations have been carried out on heat exchangers and heat transfer from extended surfaces, see for example [11,12]. Vertical fins with various shapes were considered in these studies, such as rectangular, triangular, convex parabolic and concave parabolic fins, attached to a planar wall. The fin shape considered here is another, practical and convenient, alternative which ultimately approximates well the rectangular fin shape when the fins are relatively long or thin. Further, it also has the advantages of mathematical convenience and possibility of a more accurate prediction of such quantities as the heat transfer coefficient and the heat flux along the fin and the total heat transfer from the fin.

2. Physical model and governing equations

The physical configuration of the problem under investigation is shown schematically in Fig. 1. We consider a vertical plate fin surrounded by a porous medium, which is attached to a solid base and it extends in the direction normal to the plane of the base of the fin. The vertical fin is composed of a rectangular part of thickness a and length b, to the lower part of which a half cylindrically shaped solid part of diameter a is at-

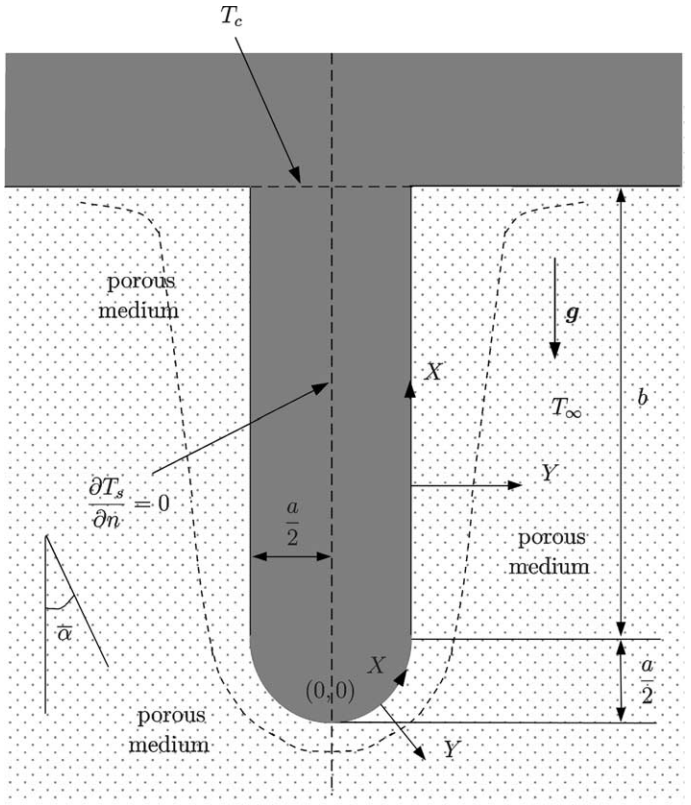

Fig. 1. Physical model, notation and coordinate system employed.

tached. This half cylindrically shaped part of the fin makes it possible to avoid the necessity of prescribing a boundary condition at the tip of the fin. In the work by Vaszi et al. [9] it was assumed that the heat loss from the end face of the fin is negligible, but this is an assumption that is only valid if the fin is very long.

For convenience, the coordinate system is chosen such that X measures the distance along the surface of the fin from the lowest point and being measured positive along the right hand side of the fin. The coordinate Y is the distance normally outwards from the fin. Further, $\bar{\alpha}(X)$ is the angle between the Y-axis and the downward vertical. As the problem is symmetrical with the axis of symmetry along the vertical centre line through the fin, we will consider in the analysis only the right hand side of the axis of symmetry.

The boundary-layer approximation is considered. Thus we assume that a boundary-layer develops around the fin, which has a finite thickness below the lowest point, i.e. the tip of the fin at $(X, Y) = (0, 0)$, and then grows in thickness with increasing values of X. The flow is assumed to be governed by the boundary-layer equations appropriate to Darcy flow. Using $X = \bar{\alpha}\frac{a}{2}$, then the Darcy equation can be expressed as follows, see [10]:

$$U = \frac{K\rho_\infty \beta g}{\mu}(T_f - T_\infty)S(X), \tag{1}$$

where U is the velocity component along the X-axis, T_f is the temperature of the porous medium, K is the permeability of the isotropic porous medium, ρ is the density of the fluid, β is the coefficient of thermal expansion, g is magnitude of the acceleration due to gravity, μ is the dynamic viscosity of the fluid and the subscript ∞ denotes the reference value at a large distance from the fin. The function $S(x)$ is defined as follows:

$$S(X) = \begin{cases} \sin\frac{2X}{a} & \text{if } 0 \leqslant X \leqslant \frac{a\pi}{4}, \\ 1 & \text{if } \frac{a\pi}{4} < X \leqslant \frac{a\pi}{4} + b, \end{cases} \tag{2}$$

and for other shaped fin tips then the function $S(X)$ will, of course, be different. The continuity equation and the energy equation may be expressed as follows:

$$\frac{\partial U}{\partial X} + \frac{\partial V}{\partial Y} = 0 \tag{3}$$

and

$$U\frac{\partial T_f}{\partial X} + V\frac{\partial T_f}{\partial Y} = \alpha\frac{\partial^2 T_f}{\partial Y^2}, \tag{4}$$

respectively. Here V is the velocity component along the Y-axis, and α denotes the effective thermal diffusivity of the porous medium. The boundary conditions for the boundary-layer flow are the following:

$$V = 0, \quad T_f = T_s \quad \text{on } Y = 0, \tag{5a}$$

$$U \to 0, \quad T_f \to T_\infty \quad \text{as } Y \to \infty, \tag{5b}$$

where T_s is the temperature in the solid fin.

By defining the streamfunction Ψ as $U = \frac{\partial \Psi}{\partial Y}$, $V = -\frac{\partial \Psi}{\partial X}$, the continuity equation (3) is satisfied identically, and the boundary-layer equations (1) and (4) transform to:

$$\frac{\partial \Psi}{\partial Y} = \frac{K\rho_\infty \beta g}{\mu}(T_f - T_\infty)S(X), \tag{6}$$

$$\frac{\partial \Psi}{\partial Y}\frac{\partial T_f}{\partial X} - \frac{\partial \Psi}{\partial X}\frac{\partial T_f}{\partial Y} = \alpha \frac{\partial^2 T_f}{\partial Y^2}, \tag{7}$$

respectively, whilst the boundary conditions (5) now become:

$$\Psi = 0, \quad T_f = T_s \quad \text{on } Y = 0, \tag{8a}$$

$$\frac{\partial \Psi}{\partial Y} \to 0, \quad T_f \to T_\infty \quad \text{as } Y \to \infty. \tag{8b}$$

We now introduce the non-dimensional variables:

$$x = \frac{X}{b}, \quad y = Ra^{1/2}\frac{Y}{b}, \quad \psi = Ra^{-1/2}\frac{\Psi}{\alpha}, \quad \theta_f = \frac{T_f - T_\infty}{T_c - T_\infty}, \quad \theta_s = \frac{T_s - T_\infty}{T_c - T_\infty}, \tag{9}$$

where Ra is defined as $Ra = \frac{gK\beta\rho_\infty(T_c - T_\infty)b}{\alpha\mu}$, and T_c is the constant heating temperature at the base of the fin. Thus Eqs. (6) and (7) are now expressed as follows:

$$\frac{\partial \psi}{\partial y} = \theta_f S(x), \tag{10}$$

$$\frac{\partial \psi}{\partial y}\frac{\partial \theta_f}{\partial x} - \frac{\partial \psi}{\partial x}\frac{\partial \theta_f}{\partial y} = \frac{\partial^2 \theta_f}{\partial y^2}, \tag{11}$$

whilst the boundary conditions (8) become

$$\psi = 0, \quad \theta_f = \theta_s \quad \text{on } y = 0, \tag{12a}$$

$$\frac{\partial \psi}{\partial y} \to 0, \quad \theta_f \to 0 \quad \text{as } y \to \infty. \tag{12b}$$

The function $S(x)$ for the present geometry is defined as follows:

$$S(x) = \begin{cases} \sin\frac{2x}{\lambda} & \text{if } 0 \leqslant x \leqslant \frac{\lambda\pi}{4}, \\ 1 & \text{if } \frac{\lambda\pi}{4} < x \leqslant \frac{\lambda\pi}{4} + 1, \end{cases} \tag{13}$$

with $\lambda = \frac{a}{b}$ being the aspect ratio of the rectangular part of the fin.

For the purpose of the analytical development and the ultimate numerical solution, we now introduce the following similarity variables:

$$\psi(x,y) = \left(2\int_0^x S(t)\,dt\right)^{1/2} F(x,\eta), \quad \theta_f(x,y) = G(x,\eta), \quad \eta = \frac{yS(x)}{\left(2\int_0^x S(t)\,dt\right)^{1/2}}. \tag{14}$$

These variables were first introduced by Merkin [10] for the free convection boundary-layer problem of a constant wall temperature from two-dimensional bodies of arbitrary shape embedded in a porous medium. On introducing expressions (13) into the expressions (14), we obtain the following:

$$\psi(x,y) = \begin{cases} \sqrt{2\lambda}\sin\frac{x}{\lambda}F(x,\eta) & \text{if } 0 \leqslant x \leqslant \frac{\lambda\pi}{4}, \\ \sqrt{\lambda\left(1-\frac{\pi}{2}\right) + 2xF(x,\eta)} & \text{if } \frac{\lambda\pi}{4} < x \leqslant \frac{\lambda\pi}{4} + 1, \end{cases}$$

$$\theta_f(x,y) = G(x,\eta), \tag{15}$$

$$\eta = \begin{cases} \sqrt{\frac{2}{\lambda}}y\cos\frac{x}{\lambda} & \text{if } 0 \leqslant x \leqslant \frac{\lambda\pi}{4}, \\ y\Big/\sqrt{\lambda\left(1-\frac{\pi}{2}\right) + 2x} & \text{if } \frac{\lambda\pi}{4} < x \leqslant \frac{\lambda\pi}{4} + 1, \end{cases}$$

and thus in terms of the variables F, G and η, Eqs. (10) and (11) transform to

$$F' - G = 0, \tag{16}$$

and

$$G'' + FG' = \lambda\tan\left(\frac{x}{\lambda}\right)\left(F'\frac{\partial G}{\partial x} - G'\frac{\partial F}{\partial x}\right) \quad \text{if } 0 \leqslant x \leqslant \frac{\lambda\pi}{4}, \tag{17}$$

$$G'' + FG' = \left(\lambda\left(1-\frac{\pi}{2}\right) + 2x\right)\left(F'\frac{\partial G}{\partial x} - G'\frac{\partial F}{\partial x}\right) \quad \text{if } \frac{\lambda\pi}{4} < x \leqslant \frac{\lambda\pi}{4} + 1, \tag{18}$$

respectively, whilst the boundary conditions (12) now become

$$F = 0, \quad G = \theta_s \quad \text{on } \eta = 0, \tag{19a}$$

$$F' \to 0, \quad G \to 0 \quad \text{as } \eta \to \infty, \tag{19b}$$

where primes denote differentiation with respect to η.

In order to model the heat conduction in the fin, the two-dimensional steady state heat conduction equation, $\nabla^2 T_s = 0$ is employed.

We consider separately the half cylindrical and the rectangular parts of the solid fin, and thus in the cylindrical part in terms of the plane polar coordinates (R, Φ), where $R = Y + \frac{a}{2}$ and $\Phi = \frac{2}{a}X - \frac{\pi}{2}$, the following equation is obtained:

$$\left(Y + \frac{a}{2}\right)^2\frac{\partial^2 T_s}{\partial Y^2} + \left(Y + \frac{a}{2}\right)\frac{\partial T_s}{\partial Y} + \frac{a^2}{4}\frac{\partial^2 T_s}{\partial X^2} = 0. \tag{20}$$

The polar coordinate system (R, Φ) has its origin at $Y = -\frac{a}{2}$, and thus the cylindrical part of the fin is in the region $0 \leqslant R \leqslant \frac{a}{2}$, $-\frac{\pi}{2} \leqslant \Phi \leqslant 0$, that is $-\frac{a}{2} \leqslant Y \leqslant 0$,

$0 \leqslant X \leqslant \frac{a\pi}{4}$. The heat flux continuity condition is applied at the porous medium–solid interface at $Y = 0$ and at the transition line between the circular and the rectangular part, i.e. at $X = \frac{a\pi}{4}$, whilst the condition of the continuity of the temperature at $X = \frac{a\pi}{4}$, and a symmetry condition at the vertical symmetry axis are also applied. Therefore the boundary conditions are the following:

$$k_s \frac{\partial T_s}{\partial Y} = k_f \frac{\partial T_f}{\partial Y} \quad \text{on } Y = 0,\ 0 \leqslant X \leqslant \frac{a\pi}{4}, \tag{21a}$$

$$(T_s)_{circ} = (T_s)_{rect} \quad \text{on } Y = -\frac{a}{2},\ 0 \leqslant X \leqslant \frac{a\pi}{4}, \tag{21b}$$

$$\frac{\partial T_s}{\partial X} = 0 \quad \text{on } X = 0,\ -\frac{a}{2} \leqslant Y \leqslant 0, \tag{21c}$$

$$\left.\begin{array}{l} (T_s)_{circ} = (T_s)_{rect} \\ \left(\frac{\partial T_s}{\partial X}\right)_{rect} = \frac{1}{\left(Y+\frac{a}{2}\right)} \frac{a}{2} \left(\frac{\partial T_s}{\partial X}\right)_{circ} \end{array}\right\} \quad \text{on } X = \frac{a\pi}{4},\ -\frac{a}{2} \leqslant Y \leqslant 0, \tag{21d}$$

where k_s and k_f are the thermal conductivities of the solid fin and the porous medium, respectively, and the notations $(\ )_{circ}$ and $(\ )_{rect}$ refer to the circular and the rectangular parts of the fin, respectively.

In order to express Eq. (20) for the temperature in the fin in non-dimensional form, the variables (9) are employed, but now the distance Y is normalized as follows:

$$\bar{y} = \frac{Y}{b}. \tag{22}$$

Thus Eq. (20) is expressed as follows:

$$\left(\bar{y} + \frac{\lambda}{2}\right)^2 \frac{\partial^2 \theta_s}{\partial \bar{y}^2} + \left(\bar{y} + \frac{\lambda}{2}\right) \frac{\partial \theta_s}{\partial \bar{y}} + \frac{\lambda^2}{4} \frac{\partial^2 \theta_s}{\partial x^2} = 0. \tag{23}$$

On applying the transformations (15) for the porous medium region, the boundary conditions (21) transform as follows:

$$\frac{\partial \theta_s}{\partial \bar{y}} = \frac{Ra^{1/2}}{\bar{k}} \sqrt{\frac{2}{\lambda}} \cos\left(\frac{x}{\lambda}\right) G' \quad \text{on } \bar{y} = 0,\ 0 \leqslant x \leqslant \frac{\lambda\pi}{4}, \tag{24a}$$

$$(\theta_s)_{circ} = (\theta_s)_{rect} \quad \text{on } \bar{y} = -\frac{\lambda}{2},\ 0 \leqslant x \leqslant \frac{\lambda\pi}{4}, \tag{24b}$$

$$\frac{\partial \theta_s}{\partial x} = 0 \quad \text{on } x = 0,\ -\frac{\lambda}{2} \leqslant \bar{y} \leqslant 0, \tag{24c}$$

$$\left.\begin{array}{l} (\theta_s)_{circ} = (\theta_s)_{rect} \\ \left(\frac{\partial \theta_s}{\partial x}\right)_{rect} = \frac{1}{\left(\bar{y}+\frac{\lambda}{2}\right)} \frac{\lambda}{2} \left(\frac{\partial \theta_s}{\partial x}\right)_{circ} \end{array}\right\} \quad \text{on } x = \frac{\lambda\pi}{4},\ -\frac{\lambda}{2} \leqslant \bar{y} \leqslant 0, \tag{24d}$$

where $\bar{k} = k_s/k_f$.

In the rectangular part of the fin, the two-dimensional steady state heat conduction equation is given as follows:

$$\frac{\partial^2 T_s}{\partial X^2} + \frac{\partial^2 T_s}{\partial Y^2} = 0, \tag{25}$$

which has to be solved subject to the following boundary conditions:

$$k_s \frac{\partial T_s}{\partial Y} = k_f \frac{\partial T_f}{\partial Y} \quad \text{on } Y = 0,\ \frac{a\pi}{4} \leqslant X \leqslant \frac{a\pi}{4} + b, \tag{26a}$$

$$\frac{\partial T_s}{\partial Y} = 0 \quad \text{on } Y = -\frac{a}{2},\ \frac{a\pi}{4} \leqslant X \leqslant \frac{a\pi}{4} + b, \tag{26b}$$

$$\left.\begin{array}{l} (T_s)_{circ} = (T_s)_{rect} \\ \left(\frac{\partial T_s}{\partial X}\right)_{rect} = \frac{1}{\left(Y+\frac{a}{2}\right)} \frac{a}{2} \left(\frac{\partial T_s}{\partial X}\right)_{circ} \end{array}\right\} \quad \text{on } X = \frac{a\pi}{4},\ -\frac{a}{2} \leqslant Y \leqslant 0, \tag{26c}$$

$$T_s = T_c \quad \text{on } X = \frac{a\pi}{4} + b,\ -\frac{a}{2} \leqslant Y \leqslant 0. \tag{26d}$$

Using the transformations (9), (15) and (22), Eq. (25) becomes

$$\frac{\partial^2 \theta_s}{\partial x^2} + \frac{\partial^2 \theta_s}{\partial \bar{y}^2} = 0, \tag{27}$$

and the boundary conditions (26) become the following:

$$\frac{\partial \theta_s}{\partial \bar{y}} = \frac{Ra^{1/2}}{\bar{k}} \frac{1}{\sqrt{\lambda\left(1 - \frac{\pi}{2}\right) + 2x}} G' \quad \text{on } \bar{y} = 0,\ \frac{\lambda\pi}{4} \leqslant x \leqslant \frac{\lambda\pi}{4} + 1, \tag{28a}$$

$$\frac{\partial \theta_s}{\partial \bar{y}} = 0 \quad \text{on } \bar{y} = -\frac{\lambda}{2},\ \frac{\lambda\pi}{4} \leqslant x \leqslant \frac{\lambda\pi}{4} + 1, \tag{28b}$$

$$\left.\begin{array}{l} (\theta_s)_{circ} = (\theta_s)_{rect} \\ \left(\frac{\partial \theta_s}{\partial x}\right)_{rect} = \frac{1}{\left(\bar{y}+\frac{\lambda}{2}\right)} \frac{\lambda}{2} \left(\frac{\partial \theta_s}{\partial x}\right)_{circ} \end{array}\right\} \quad \text{on } x = \frac{\lambda\pi}{4},\ -\frac{\lambda}{2} \leqslant \bar{y} \leqslant 0, \tag{28c}$$

$$\theta_s = 1 \quad \text{on } x = \frac{\lambda\pi}{4} + 1,\ -\frac{\lambda}{2} \leqslant \bar{y} \leqslant 0. \tag{28d}$$

2.1. Physical quantities

The local heat transfer coefficient, the local heat flux and the total heat transfer rate from the fin are defined as follows:

$$h_d(X) = -k_f \left.\frac{\partial T_f}{\partial Y}\right|_{Y=0} \frac{1}{T_s(X,0) - T_\infty}, \tag{29}$$

$$q_d(X) = -k_f \left.\frac{\partial T_f}{\partial Y}\right|_{Y=0} \tag{30}$$

and

$$Q_d = 2 \int_0^{\frac{a\pi}{4}+b} q_d(X)\, dX, \tag{31}$$

respectively. In non-dimensional form, these quantities are normalised as $h(x)=\frac{h_d(X)b}{k_f Ra^{1/2}}$, $q(x)=\frac{q_d(X)b}{k_f(T_c-T_\infty)Ra^{1/2}}$ and $Q=\frac{Q_d}{k_f(T_c-T_\infty)Ra^{1/2}}$, and, via the expressions (9) and (15), they can be expressed in the following form:

$$h(x)=\begin{cases}-G'(x,0)\sqrt{\frac{2}{\lambda}}\cos\frac{x}{\lambda}\,\frac{1}{\theta_s(x,0)} & \text{if } 0\leqslant x\leqslant\frac{\lambda\pi}{4},\\ -G'(x,0)\frac{1}{\sqrt{\lambda\left(1-\frac{\pi}{2}\right)+2x}}\,\frac{1}{\theta_s(x,0)} & \text{if } \frac{\lambda\pi}{4}<x\leqslant\frac{\lambda\pi}{4}+1,\end{cases} \tag{32}$$

$$q(x)=\begin{cases}-G'(x,0)\sqrt{\frac{2}{\lambda}}\cos\frac{x}{\lambda} & \text{if } 0\leqslant x\leqslant\frac{\lambda\pi}{4},\\ -G'(x,0)\frac{1}{\sqrt{\lambda\left(1-\frac{\pi}{2}\right)+2x}} & \text{if } \frac{\lambda\pi}{4}<x\leqslant\frac{\lambda\pi}{4}+1,\end{cases} \tag{33}$$

and

$$Q=2\int_0^{\frac{\lambda\pi}{4}}\left[-G'(x,0)\sqrt{\frac{2}{\lambda}}\cos\frac{x}{\lambda}\right]\mathrm{d}x+2\int_{\frac{\lambda\pi}{4}}^{\frac{\lambda\pi}{4}+1}\frac{-G'(x,0)\,\mathrm{d}x}{\sqrt{\lambda\left(1-\frac{\pi}{2}\right)+2x}}, \tag{34}$$

respectively.

For the purpose of comparison of the results with those presented by Vaszi et al. [9], we introduce the conduction–convection parameter N_{cc}, which is defined as $N_{cc}=\frac{2Ra^{1/2}}{k\lambda}$.

3. Method of solution

The equations for the porous medium and the fin regions are both approximated by finite differences and an iterative solution procedure is implemented in which the equations are solved to convergence. This numerical procedure follows closely the method described by Vaszi et al. [13], which was also employed by Vaszi et al. [9]. Vaszi et al. [13] provided a detailed description of the method, and therefore details are not repeated here.

In the fin region, the equations for the circular and the rectangular parts have to be solved separately, subject to the appropriate boundary conditions. At the transition line between the cylindrical and the rectangular regions of the fin, i.e. at $x=\frac{\lambda\pi}{4}$, both the conditions of the continuity of the temperature and the heat flux are satisfied, see the boundary condition (24d). In the cylindrical region, the first condition from (24d) is applied, namely the continuity of the temperature, whilst in the rectangular region the second condition, i.e. the continuity of the heat flux is used.

When solving Eqs. (23) (24), (27) and (28) in the fin region, first a number of iterations are processed on the equations for the cylindrical part in order to obtain an estimate for $(\theta_s)_{circ}$ and then this estimate is used to process a number of iterations on Eqs. (27) and (28) in the rectangular part of the fin. Then, as an estimate for θ_s for the whole fin is obtained in this manner, the outer iteration continues with the solving of Eqs. (16)–(19) for the porous medium region by using this estimate.

4. Results and discussion

In this section results are presented and discussed in terms of the plate aspect ratio, λ, and the conduction–convection parameter, N_{cc}. Also, we discuss briefly the dependence of the solutions on the numerical parameters. Thus we have found that accurate numerical solutions can be obtained by setting the value of $\eta_\infty=8$ for the location of the infinity boundary in the porous medium region, 80 grid points in the η direction and the same grid points in the x direction for the fin and the porous medium regions. The iterative procedure has been continued until the maximum error for two successive iterations between the fields ψ, θ_f and θ_s became smaller than $\varepsilon=10^{-6}$. If we took $\varepsilon=10^{-7}$ then the results become indistinguishable from those presented in the paper.

Numerical results have been obtained for the values of the fin aspect ratio $\lambda=0.025$, 0.05, 0.1, 0.2 and 0.5. For $\lambda\geqslant 0.1$, in the rectangular part of the fin region the number of grid points in the x direction has been set to be 81. Then the number of the grid points in the x direction in the circular part of the fin has been set such that the step sizes along $\bar{y}=0$ from $x=0$ to $\frac{\lambda\pi}{4}+1$, and the step sizes in the $\bar{y}$ direction have about the same magnitude. However, for $\lambda=0.025$ and 0.05, it is nec-

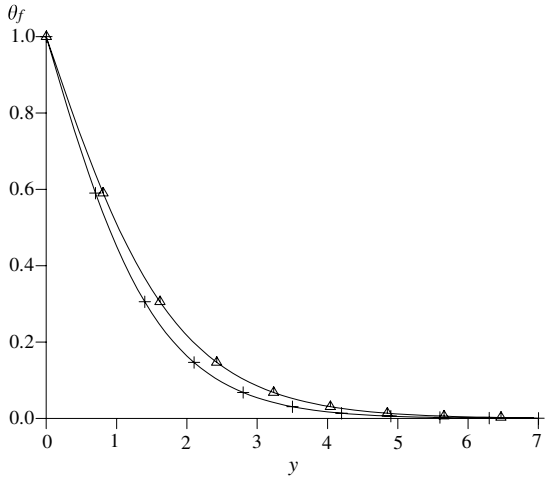

Fig. 2. The non-dimensional fluid temperature profiles, θ_f, as a function of y, when an isothermal cylinder is considered. The lines marked by + and △ show the results for $\bar{\alpha}=0°$ and $\bar{\alpha}=60°$, respectively.

essary to set larger grids, thus for $\lambda = 0.025$ the grids $(4\times3)_{\text{circ}}$ and $(121\times3)_{\text{rect}}$, whilst for $\lambda = 0.05$ the grids $(6\times4)_{\text{circ}}$ and $(121\times4)_{\text{rect}}$ have been set in the fin.

Fig. 2 shows the results for the non-dimensional temperature θ_f at $\bar{\alpha} = 0°$ and $\bar{\alpha} = 60°$ as a function of the radial distance y, when both the rectangular and the circular parts of the fin are considered to be isothermal at the non-dimensional temperature $\theta_s = 1$. The results presented in this figure agree very well with the results of Ingham et al. [14], who investigated the free convection boundary layers on an isothermal horizontal cylinder.

Fig. 3 shows results for the non-dimensional temperature on the conjugate boundary $\theta_f(x, 0)$, obtained for various values of the fin aspect ratio, λ, plotted by the continuous lines. These results are compared to those presented in Fig. 3 of the paper by Vaszi et al. [9] for a rectangular plate fin, which are shown by the dashed lines. Both for $N_{cc} = 0.5$ and 2, the temperature profiles for the fin with the rounded tip increase with decreasing values of the fin aspect ratio, and they appear to tend to a limit when $\lambda \to 0$. This limit is near to the limit which is approached by the temperature profiles plotted for the rectangular fin for small values of λ.

Fig. 4 presents results for (a) the non-dimensional local heat transfer coefficient, $h(x)$, and (b) the non-dimensional local heat flux, $q(x)$, calculated for $N_{cc} = 0.5$, 2 and 12. Results obtained for various values of the fin aspect ratio, λ, shown by the continuous lines, are compared to the results obtained by using the finite fin formulation for the rectangular fin. The latter results are only shown for $\lambda = 0.2$, plotted by the dashed lines, as the results for $\lambda \lesssim 0.2$ do not differ significantly, see [9].

It is seen, for the fin with the rounded tip, that both the non-dimensional local heat transfer coefficient and heat flux vary greatly as the fin aspect ratio decreases, and it appears that both quantities ultimately approach the result obtained by the finite fin formulation with the

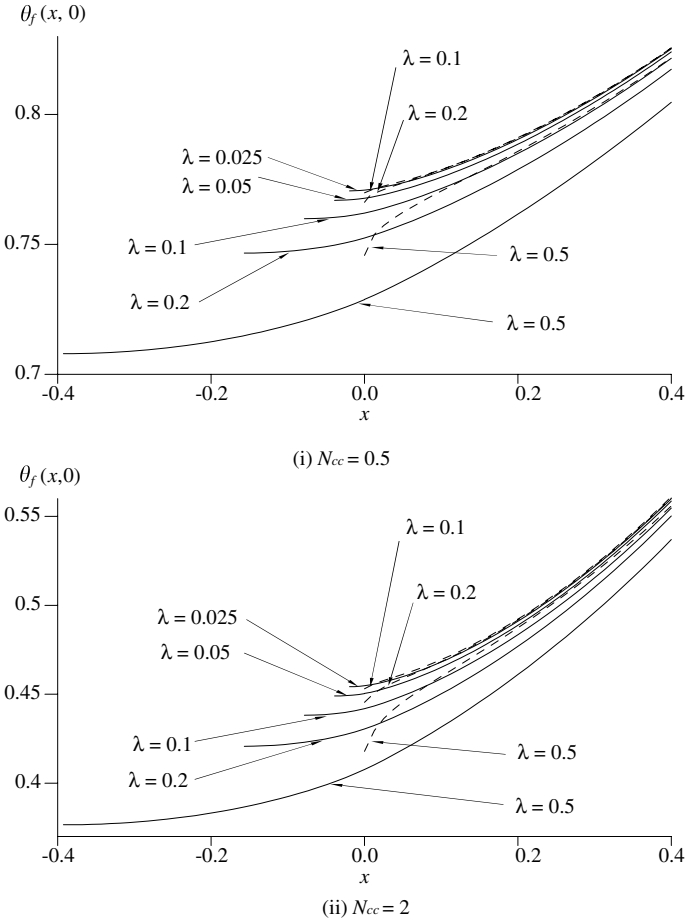

Fig. 3. The non-dimensional fluid temperature on the conjugate boundary, $\theta_f(x, 0)$, calculated for (i) $N_{cc} = 0.5$, and (ii) $N_{cc} = 2$, and for various values of the aspect ratio, λ. The continuous and the dashed lines show results obtained for the fin with a cylindrical tip, and for the rectangular fin, respectively.

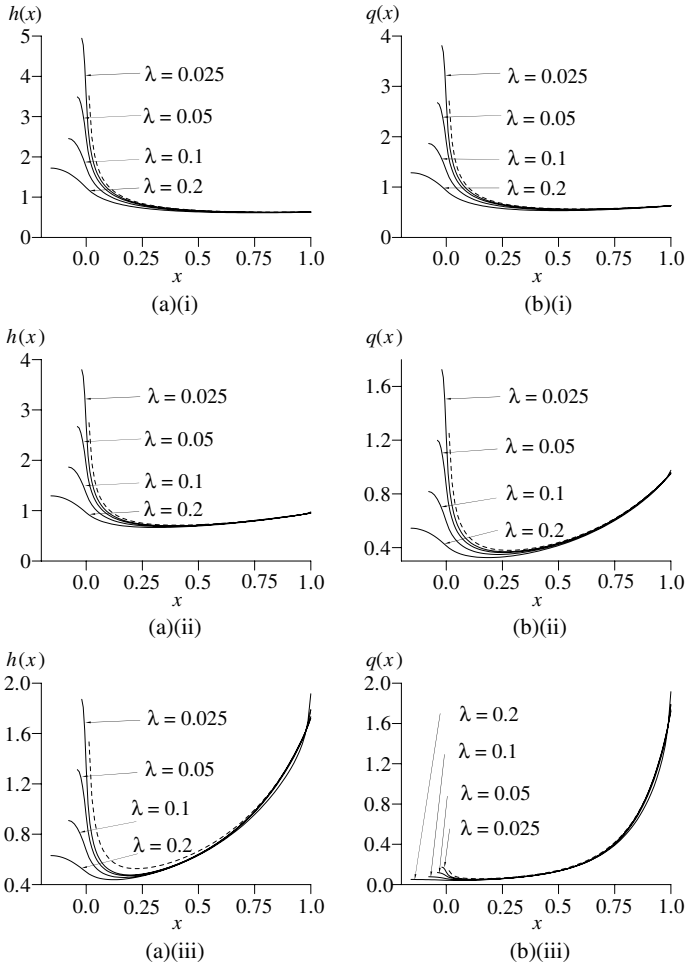

Fig. 4. (a) The non-dimensional local heat transfer coefficient, $h(x)$, and (b) the non-dimensional local heat flux, $q(x)$, calculated for (i) $N_{cc} = 0.5$, (ii) $N_{cc} = 2$ and (iii) $N_{cc} = 12$. The continuous and the dashed lines show results obtained for the fin with a cylindrical tip, and for the rectangular fin, respectively.

insulated tip, for all values of N_{cc} investigated. Also, in a similar manner to the results for the rectangular plate fin, the trend of rapidly decreasing values for $h(x)$ and $q(x)$ near the tip with increasing values of x is observed for small values of λ. However, as the aspect ratio increases, a smoother drop is observed near the tip of the fin.

In Table 1 we present the total heat transfer rate, Q, for $N_{cc} = 0.5$, 2 and 12, obtained for the values of the fin aspect ratio $\lambda = 0.025$, 0.05, 0.1 and 0.2, and the results for the rectangular plate fin are also presented for $\lambda = 0.2$. The results for Q at $\lambda = 0.2$ and for other values of λ for the rectangular plate fin are listed in Table 1 in [9].

It is observed that for all investigated values of N_{cc} the total heat transfer rate is always smaller for the rectangular plate fin than for the fin with the circular tip and this is expected as in the latter case the heat transfer surface is larger. Also, the total heat transfer rate decreases with increasing values of N_{cc}, and this is expected as increasing values of N_{cc} may be associated with decreasing values of the thermal conductivity ratio between the fin and the porous medium when λ is fixed.

Table 1
The total heat transfer rate, Q

Q	$N_{cc} = 0.5$	$N_{cc} = 2$	$N_{cc} = 12$
Rectangular fin	1.425304	1.102953	0.635799
$\lambda = 0.025$	1.472561	1.119455	0.641984
$\lambda = 0.05$	1.486228	1.124212	0.640907
$\lambda = 0.1$	1.529286	1.138419	0.632221
$\lambda = 0.2$	1.547875	1.139061	0.616232

Further, it is observed that for $N_{cc} = 0.5$ and 2 the total heat transfer rate increases as λ increases, and this is a direct consequence of the increasing heat transfer surface at the tip of the fin. However, in a rather surprising manner, this trend is not apparent for $N_{cc} = 12$, as when increasing λ and thus the heat transfer surface results in slightly lower values of Q. We postulate the reason for this is that large values of N_{cc} may again be associated with small values of the thermal conductivity of the fin, and in this case the extension of the heat transfer surface does not appear to be a major factor in influencing the total heat transfer rate. It should also be noted that the same trend of decreasing values of Q with increasing values of λ was found in the case of the rectangular plate fin, for all investigated values of N_{cc}, see Table 1 in [9]. Therefore an important conclusion is drawn, namely that increasing the heat transfer surface does not increase the total heat transfer in all circumstances.

5. Concluding remarks

In this paper the study of the two-dimensional steady state free convection from a vertical rectangular plate fin embedded in a porous medium has been extended to a vertical fin with a cylindrical tip. A boundary-layer investigation has been performed in the porous medium region, both around the cylindrical tip and next to the main body of the fin, whilst in the fin two-dimensional heat conduction has been considered. The governing parameters of the problem are identified as the conduction–convection parameter, $N_{cc} = \frac{2Ra^{1/2}}{k\lambda}$, and the aspect ratio of the fin, λ.

By attaching the cylindrical part to the tip of the fin, the problem of dealing with the heat transfer at the tip of the fin in situations when the fin is thin is mathematically naturally resolved, and it is not necessary to introduce artificial approximations, such as insulating the tip of the fin. However, for relatively large values of the aspect ratio, the problem of considering the alternatives of an insulated fin tip or a cylindrical fin tip in order to address the heat transfer at the tip of the fin in an appropriate way is of little importance, as these two alternatives are addressing different problems.

It is important to note that as the fin aspect ratio, λ, takes small values, and eventually tends to 0, the results for the non-dimensional temperature, local heat transfer coefficient, local heat flux and total heat transfer for the fin with the cylindrical tip approach those for the rectangular fin. The local heat transfer coefficient and the local heat flux show a more gradual drop along the rounded tip as the aspect ratio of the fin becomes larger. For most values of the conduction–convection parameter, N_{cc}, the total heat transfer from the fin increases with increasing values of the aspect ratio. However, a different behaviour is observed when this parameter becomes large, a situation which is associated with a low thermal conductivity ratio between the fin and the porous medium.

It should be noted that in all the results presented in this paper we have assumed that there is a rectangular part of the fin which is made smooth by adding on to the end of the fin a cylindrically shaped end. However, the work presented in this paper can easily be extended to any smoothly shaped fin.

Acknowledgements

Professors D.B. Ingham and I. Pop would like to express their thanks to the Royal Society for funding some of the work reported in this paper.

References

[1] E.M. Sparrow, A. Acharya, A natural convection fin with a solution-determined non-monotonically varying heat transfer coefficient, ASME J. Heat Transfer 103 (1981) 218–225.
[2] E.M. Sparrow, M.K. Chyu, Conjugated forced convection–conduction analysis of heat transfer in a plate fin, ASME J. Heat Transfer 104 (1982) 204–206.
[3] D.A. Nield, A. Bejan, Convection in Porous Media, Springer, New York, 1999.
[4] I. Pop, D.B. Ingham, Convective Heat Transfer: Mathematical and Computational Modelling of Viscous Fluids and Porous Media, Pergamon, Oxford, 2001.
[5] B. Sunden, P.J. Heggs (Eds.), Recent Advances in Analysis of Heat Transfer for Fin Type Surfaces, WIT Press, Southampton, Boston, 2000.
[6] I. Pop, A. Nakayama, Conjugate free and mixed convection heat transfer from vertical fins embedded in porous media, in: B. Sunden, P.J. Heggs (Eds.), Analysis of Heat Transfer for Fin Type Surfaces, Computational Mechanics Publications, Southampton, 1999, pp. 67–96 (Chapter 14).
[7] J.-Y. Liu, W.J. Minkowycz, The influence of lateral mass flux on conjugate natural convection from a vertical plate fin in a saturated porous medium, Numer. Heat Transfer 10 (1986) 507–520.
[8] J.-Y. Liu, S.-D. Shih, W.J. Minkowycz, Conjugate natural convection about a vertical cylindrical fin with lateral mass flux in a saturated porous medium, Int. J. Heat Mass Transfer 30 (1987) 623–630.
[9] A.Z. Vaszi, L. Elliott, D.B. Ingham, I. Pop, Conjugate free convection from vertical fins embedded in a porous medium, Num. Heat Transfer A 44 (2003) 743–770.
[10] J.H. Merkin, Free convection boundary layers on axisymmetric and two-dimensional bodies of arbitrary shape in a saturated porous medium, Int. J. Heat Mass Transfer 22 (1979) 1461–1462.
[11] M. Manzoor, Heat Flow Through Extended Surface Heat Exchangers, Springer-Verlag, Berlin, 1984.
[12] P.J. Heggs, D.B. Ingham, S.D. Harris, Extended Surface Conjugate Heat Transfer, John Wiley, in press.

[13] A.Z. Vaszi, L. Elliott, D.B. Ingham, I. Pop, Conjugate free convection above a heated finite horizontal flat plate embedded in a porous medium, Int. J. Heat Mass Transfer 45 (2002) 2777–2795.

[14] D.B. Ingham, J.H. Merkin, I. Pop, The collision of free-convection boundary layers on a horizontal cylinder embedded in a porous medium, Q. J. Mech. Appl. Math. 36 (1983) 313–335.